Available online at www.sciencedirect.com

ScienceDirect

Procedia CIRP 46 (2016) 396 – 399

www.elsevier.com/locate/procedia

7th HPC 2016 – CIRP Conference on High Performance Cutting

Comparison of different control strategies for active damping of heavy duty milling operations

Robin Kleinwort[a]*, Martin Schweizer[a], Michael F. Zaeh[a]

[a]*Institute for Machine Tools and Industrial Management, Technical University of Munich (TUM), Boltzmannstraße 15, 85748 Garching, Germany*

* Corresponding author. Tel.: +49-(0)89-289-15571; Fax: +49-(0)89-289-15555. *E-mail address:* Robin.Kleinwort@iwb.tum.de

Abstract

Depending on the machining process chatter might occur at an eigenfrequency of the machine's structure. Electrodynamic proof-mass actuators can be attached to the structure in order to mitigate chatter. This paper gives an overview of different existing control strategies for active damping and compares them with one another. First, the control strategies were implemented and tested in a coupled simulation model. Then, the simulation results were validated by modal tests. For a sample process the analytically predicted depths of cut were finally verified in cutting tests.

Peer-review under responsibility of the International Scientific Committee of 7th HPC 2016 in the person of the Conference Chair Prof. Matthias Putz

Keywords: Machine tool; Chatter; Control; Active Damping

1. Introduction

The maximum material removal rate of machine tools is determined by either the drive capacity of the spindle or - more often - by the stability limit. Under certain conditions the machining process can become instable and chatter occurs. Chatter causes high dynamic forces on the machine's bearings, a poor surface finish and high tool wear.

The active vibration control (AVC) system used in this research is able to mitigate chatter caused by the eigenmodes of the machine tool's structure except the spindle shaft or the tool. This publication focuses on the comparison of several control strategies used for active damping.

A very popular approach is to use collocated control strategies as proposed by [1,2]. Collocated control is characterized by collocated actuator and sensor pairs. One widely-used possibility for collocated control is the direct velocity feedback (DVF) controller, successfully tested in cutting tests by [3,6].

Another method often used for disturbance rejection purposes are model based linear quadratic regulators (LQR), usually in combination with state space observers, as proposed by [1] and successfully deployed on machine tools by [4,5].

The last two control strategies considered in this paper belong to the field of robust control. H_∞-control considers unstructured uncertainties and robust stability demands in the design process [2]. If structured uncertainties occur, µ-synthesis control should be used, which also considers robust performance demands. There exist several approaches for both robust control strategies to use them for active damping of machine tools [2,4].

For the first time, this paper compares the performance of these different control strategies in modal and cutting tests.

2. Active damping system

Fig. 1 shows the collocated placement of the main components: the actuator (SA10-V30 by CSA Engineering) and the acceleration sensor (KS 813B by MMF). They are placed in an antinode of the machine's most critical eigenmode. The actuator is driven by an amplifier (BAA 120 by BEAK) and as a proof-mass actuator it can be attached to the machine's structure at any arbitrary position.

Peer-review under responsibility of the International Scientific Committee of 7th HPC 2016 in the person of the Conference Chair Prof. Matthias Putz
doi:10.1016/j.procir.2016.04.054

The control rule is implemented on a rapid prototyping system (MicroLabBox by dSpace) with a sample frequency of 10 kHz.

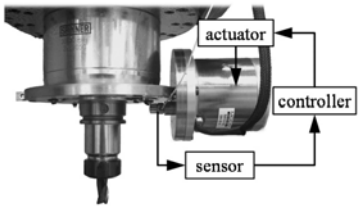

Fig. 1. machine tool with actuator and sensor.

3. Simulation model

The simulation model consists of two components: one model for the mechanical structure of the machine tool and one model for the actuator unit, which includes the actuator itself and the amplifier. Because of its almost ideal transfer characteristics the sensor transfer function was neglected in the modelling process.

The model of the mechanical structure of the machine tool was obtained via experimental modal analysis. It includes the first five eigenmodes of the machine tool. The behavior of the machine tool is described by a second order differential equation, where $[M]$, $[D]$ and $[K]$ are the mass, damping and stiffness matrix respectively, $\{q\}$ the displacements in Cartesian coordinates and $\{F\}$ the applied forces:

$$[M]\{\ddot{q}\}+[D]\{\dot{q}\}+[K]\{q\}=\{F\}. \tag{1}$$

Following [1], the transfer function of a proof-mass actuator can be described in the form of:

$$G_A(s)=g_A\,\frac{s^2}{s^2+2\zeta_A\omega_A s+\omega_A^2}, \tag{2}$$

with g_A being the gain factor, ζ_A the damping factor and ω_A the natural eigenfrequency of the actuator. In order to identify the parameters in eq. (2) the transfer function of the actuator unit was determined experimentally. As fig. 2 depicts, not only the transfer function of the actuator itself but the transfer function of the actuator unit consisting of actuator and amplifier could be approximated very well in the relevant frequency range (20-200 Hz) after adjusting the parameters.

Both models for the mechanical structure of the machine tool and the actuator unit were consolidated in a state space model of the form:

$$\begin{aligned}\{\dot{x}\}&=[A]\{x\}+[B]\,u,\\ y&=[C]\{x\}+[D]\,u,\end{aligned} \tag{3}$$

where $[\boldsymbol{A}]$, $[\boldsymbol{B}]$, $[\boldsymbol{C}]$ and $[D]$ are the system matrix, input matrix, output matrix and transition matrix respectively. u is the input quantity, in this case the control voltage at the actuator unit. On the other hand, y is the output quantity, which is the measured acceleration at the sensor position. The state vector $\{x\}=\{\{\boldsymbol{q_m}\},\{\dot{\boldsymbol{q}}_{\boldsymbol{m}}\},\{\boldsymbol{x_A}\}\}$ includes the states of the mechanical structure in modal coordinates $\{\boldsymbol{q_m}\}$ and the states of the actuator unit $\{\boldsymbol{x_A}\}$.

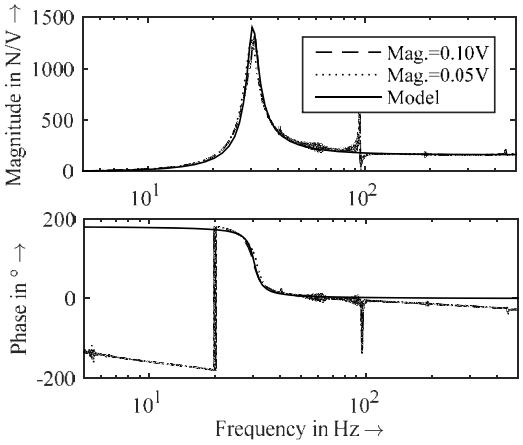

Fig. 2. actuator transfer function at two magnitudes and the identified model.

4. Control strategies for active damping of machine tools

In the following section the basics of collocated, optimal and robust control are presented.

4.1. Collocated control

Compared to other collocated control strategies, the DVF controller shows the best performance on machine tools [6]. Collocation between the actuator and the sensor leads to higher stability of the control loop [1]. A velocity feedback controller acts as a viscous damper by applying an actuator force F_{act} proportional to the measured velocity signal to the system:

$$F_{act}=-K_C\dot{x}, \tag{4}$$

where the gain K_C is the only variable, which has to be adapted in a way that the controller remains stable.

4.2. Optimal control

Optimal control is characterized by the desire to control a dynamic system at minimum cost. If the system can be described by a set of linear differential equations and the cost by a quadratic equation, the problem can be solved by the linear-quadratic regulator (LQR). The cost function, which has to be minimized, is:

$$J=\frac{1}{2}\int_0^\infty x^T Q\,x+u^T R\,u\,dt, \tag{5}$$

where Q and R are - usually diagonal - weight matrices. It has two contributions: The first one is the term $x^T Qx$, which makes sure that the controlled state space vector entries approach zero after an initial displacement in a speed corresponding to their

respective weight. The second one is the term $u^T Ru$, which is in a similar manner responsible for keeping the control input in the control process as small as possible.

In comparison to the DVF controller, the LQR can be tuned to focus on damping only certain eigenmodes. Placing a high weight on the first state space vector entry for example yields a controller, which leads to damping the corresponding first eigenmode.

The LQR is a state space control method, which means that the feedback is obtained by multiplying the state space vector $x(t)$ with a matrix $[K]$:

$$u(t) = -Kx(t). \tag{6}$$

In the case described in this paper the state space vector cannot be measured without great effort. Therefore, the LQR is extended with a Kalman observer in order to estimate the states, which turns it into a linear-quadratic-Gaussian (LQG) controller.

4.3. Robust control

The dynamic behavior of the machine tool depends to a great extent on the position of the tool. With robust control the uncertainties in the simulation model can be considered in the control design process. A distinction must be made between unstructured and structured uncertainties. Unstructured uncertainties describe the uncertainties of a structural model directly in its frequency response characteristics, e.g. in multiplicative form:

$$G(s)=G_n(s)\cdot(I+W_m(s)\,\Delta_u(s)),\|\Delta_u(s)\|_\infty \le 1, \tag{7}$$

with the nominal transfer function $G_n(s)$, a weight function $W_m(s)$ and an arbitrary norm bounded transfer function $\Delta_u(s)$. Structured uncertainties, which are considered only in µ-synthesis, can be used to model parameter uncertainties (e.g. uncertain damping parameters etc.):

$$d = d_n\cdot(1+d_v\delta_s),|\delta_s|\le 1. \tag{8}$$

In the H_∞-control and µ-synthesis design process weight transfer functions are added to the feedback loop consisting of the structural model G and the controller K, which leads to the generalized structural model P with an additional performance channel from w to z (Fig. 3 (a)). The idea of H_∞-control and µ-synthesis is to find a controller K, which stabilizes the closed loop and minimizes the worst case energy transfer from the exogenous input w to the error signals z or in other words minimizes the H_∞-norm of the transfer function T_{zw}:

$$\| T_{zw} \|_\infty \le 1. \tag{9}$$

If such a controller can be found, the sensitivity functions of the nominal closed loop are bounded by the inverse of their respective weight functions. In this paper the weighting scheme according to [2] was used.

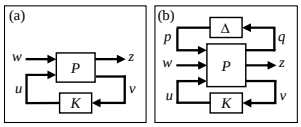

Fig. 3. (a) generalized structural model P; (b) generalized structural model P with uncertainty block.

In H_∞-control the demand for robust stability can be taken into account as a demand for nominal performance, whereas in µ-synthesis the structured and unstructured uncertainties are directly considered for the block diagram in Fig. 3 (b).

Robust stability is satisfied in µ-theory, if the greatest µ-value of the closed loop transfer function of P and K with regard to the uncertainty block Δ is equal to or smaller than one for $||\Delta||_\infty < 1$.

5. Simulation results

Fig. 4 shows the simulated receptance frequency response function (FRF) at the TCP with the different control strategies compared to the machine's dynamics without active damping. The following results were achieved on a SPINNER U5-620 machining center. For reasons of confidentiality, all receptance FRFs are normalized. The first eigenfrequency around 20 Hz refers to the rigid-body mode, which is irrelevant for the chatter stability. The controller settings were chosen in a way that the highest damping of the 60 Hz eigenmode is achieved, while still remaining stable in experiments. Global convergence is not guaranteed for the optimization method used in µ-synthesis, so the resulting controller can depend on the start-value. In this case no µ-controller could be found, which satisfies the desired robust performance specification for the modeled structured uncertainties, however µ-synthesis with the previously calculated H_∞-controller as start-value has shown that the H_∞-controller yields a local minimum.

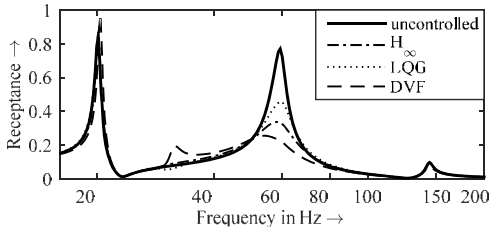

Fig. 4. simulated receptance FRF at the TCP in model reference position.

Because of model inaccuracies the achievable performance of the LQG and the H_∞ controller in damping the 60 Hz mode is not as good as for the non-model based DVF controller.

Unfortunately, the DVF controller amplifies the rigid-body motion at 22 Hz due to a high phase shift of the controller at this frequency. Furthermore, the DVF controller shows a higher receptance at 33 Hz, which refers to the eigenfrequency of the actuator. The H_∞ and the LQG controller only damp the eigenmode at 60 Hz and show no unwanted amplification at any other frequency. In theory the performance of the LQG controller is expected to be higher at the model reference

position as the H_∞ also has to fulfill robust stability. However, in experiments the H_∞ is more stable, which allows to use more aggressive control settings. Therefore, the H_∞ achieves a higher damping than the LQG controller. Because of model inaccuracies the achievable performance of both controllers in damping the 60 Hz mode is limited compared to the non-model based DVF controller.

6. Experimental results

Using the same control settings as in chapter 5, the receptance FRF was measured at the TCP in machine x-direction with an impulse hammer (9726A5000 by KISTLER) and an acceleration sensor (KS 813B by MMF). According to fig. 4 and fig. 5 the simulation results are in good agreement with the measurements. For all controllers the expected performance was surpassed. A reason for this might be inaccuracies in the modeled actuator transfer function. The H_∞ -controller shows an unexpected amplification of the actuator eigenfrequency at 33 Hz in fig. 5.

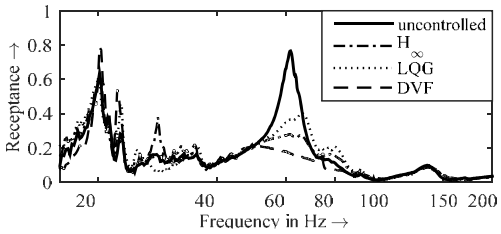

Fig. 5. receptance FRF at the TCP in model reference position.

When changing the machine position, the machine's dynamics change, too. In fig. 6 the receptance FRF at the TCP in x-direction is shown for another machine position. Due to strong deviations between the model and the new machine position, the LQG controller amplifies the mode at 80 Hz instead of damping it. The H_∞ and the DVF controller both show good results, according to fig. 6. It seems that the DVF controller performs best in damping the dominant mode, but it has to be mentioned that this control strategy is very sensitive to low frequency noise. In case of high feed drive acceleration for example, the measured signal can lead to a saturation of the actuator and the controller can even become instable.

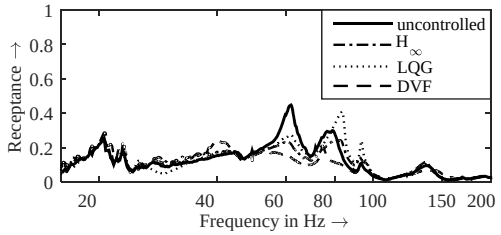

Fig. 6. receptance FRF at the TCP in a position different than model reference position.

Using the measured receptance FRFs in fig. 5, the maximum stable depths of cut for the different control strategies at the reference position were calculated with the software CutPro from MALINC for a slotting operation with a D=50mm shoulder mill. After that, cutting tests were performed with unalloyed steel C45 to validate the maximum stable depths of cut. The results are summarized in table 1.

Table 1. maximum stable depths of cut for the different control strategies.

Control strategy	No AVC	DVF	LQG	H_∞
CutPro	1.5 mm	3.7 mm	2.7 mm	3.2 mm
Cutting tests	1.5 mm	2.9 mm	2.4 mm	2.9 mm
Increase in %	0%	93%	60%	93%

The LQG controller is falling short of the expected depth of cut calculated in CutPro. With the DVF and the H_∞-controller the material removal rate respectively the depth of cut was increased up to the maximum spindle power. A higher depth of cut might have been possible but could not be tested in cutting tests due to the spindle power limit.

7. Summary

The simulation model presented in this paper is able to test the performance of different active damping control strategies. Validation experiments showed only small deviations between the simulated and measured receptance FRF. The LQG controller achieved the smallest increase of the maximum stable depth of cut. Furthermore, the modal tests showed that the LQG controller has difficulties when the machine's dynamics change. Therefore, in future work the focus will be on the DVF controller as well as the H_∞- and the μ-synthesis controller. Further cutting tests with multi-axis machining as well as different immersion angles have to be performed to evaluate the capability of these control strategies for active damping of machine tools in industry.

Acknowledgements

The authors would like to thank the Bayerisches Staatsministerium für Wissenschaft, Forschung und Kunst (StMWFK) for funding the project E²D within the joint project 'Green Factory Bavaria'.

References

[1] Preumont A. Vibration Control of Active Structures – An Introduction. 2nd ed. Dordrecht: Kluwer Academic Publishers, 2002.
[2] Schönhoff U. Practical Robust Control of Mechatronic Systems with Structural Flexibilities. Dissertation, TU Darmstadt, 2003.
[3] Baur M, Zaeh, MF. Development and Experimental Validation of an Active Vibration Control System for a Portal Milling Machine. Proceedings of 9th International Conference on High Speed Machining, San Sebastian, 2012.
[4] Kern S. Erhöhung der Prozessstabilität durch aktive Dämpfung von Frässpindeln mittels elektromagnetischer Aktoren. Dissertation, TU Darmstadt, 2009.
[5] Simnofske M. Adaptronische Versteifung von Werkzeugmaschinen durch strukturintegrierte aktive Module. Dissertation, TU Braunschweig, 2009.
[6] Munoa J, Mancisidor I, Loix N, Uriarte L, Barcena R, Zatarain M. Chatter suppression in ram type travelling column milling machines using a biaxial inertial actuator. CIRP Annals – Manufacturing Technology 2013; 62:407-410.